

# Particle formation and agglomeration of an alumina–zirconia powder synthesized an supercritical CO<sub>2</sub> method

Hasan Gocmez <sup>a,\*</sup>, Mustafa Tuncer <sup>a</sup>, Ismail Uzulmez <sup>a</sup>, Osman Sahin <sup>b</sup>

<sup>a</sup> Department of Ceramic Engineering, Dumlupinar University, Kutahya, Turkey

<sup>b</sup> Department of Physics, Mustafa Kemal University, Hatay, Turkey

Received 15 February 2011; received in revised form 23 April 2011; accepted 4 August 2011

Available online 2 September 2011

## Abstract

Alumina – 20 vol% zirconia doped with 2 mol% yttria composites were prepared by a supercritical CO<sub>2</sub> method. The powder characteristics were examined through control of the supercritical conditions; temperature and pressure. The agglomeration degrees (N) for powders were changed from 1.2 and 5.4. As the value N become smaller or close to unity, powder agglomerates tend to approach their primary powder size. The sintered sample had hardness of 12.5 GPa. SEM and TEM characterization were used to characterize the microstructure and morphology of the prepared powders.

© 2011 Elsevier Ltd and Techna Group S.r.l. All rights reserved.

**Keywords:** A. Powders: chemical preparation; B. Nanocomposites; D. Al<sub>2</sub>O<sub>3</sub>; D. ZrO<sub>2</sub>

## 1. Introduction

Research on the synthesis of nanocomposite materials have accelerated recently due to the specific engineering properties requirements of materials for structural and functional application [1]. Among these materials, alumina–zirconia composites (ZTA) are well-known structural materials owing to their excellent strength, toughness, thermal shock and superior wear resistance properties. The wide applications of these composites include structural materials for high-temperature gas burners, cutting tools, ball bearing, biomaterials, catalytic support, etc. [2–4].

Various synthesis techniques have been described in the literature for preparing alumina–zirconia powders. These techniques include colloidal processing [5], solution combustion [6] coprecipitation [7], chemical vapor deposition [8] and sol–gel synthesis [9]. In recent years, the supercritical fluids have also been used for the synthesis of powders as a particle-forming media due to their unique properties, such as their high diffusivities, low surface tension and liquid like densities. The powder properties are continuously variable by manipulation of

the pressure and temperature within the reaction vessel, which allows a tailoring of the fluid properties to improve the formation of nanocrystalline powders. A fluid reaches a supercritical state when it is above its critical temperature and pressure. In this state, it has a single phase (no phase boundary between liquid and gas) having combination of gas like (viscosity, diffusion coefficient) and liquid like (density) properties [10–13].

The synthesis of powders by supercritical fluids is a method involving formation of precipitation formed by contacting precursor solutions with supercritical fluid at elevated temperature in a pressurized vessel. The water, alcohols or carbon dioxide are used as supercritical fluid media in powder formation. Among these fluids, carbon dioxide is most attractive due to chemically stable, environmentally benign, non-flammable, cheaper and non-toxic. It also reaches its supercritical state at low critical temperature (31 °C) and pressure (7.38 MPa). Furthermore, when reaction is carried out in supercritical CO<sub>2</sub>, reaction products can be easily recovered by simply venting the solvent [14,15].

As far as we are aware, there has not been any report for preparing alumina–zirconia powder using the supercritical CO<sub>2</sub> method. In this study, we use supercritical CO<sub>2</sub> in GAS method to synthesis (80/20 vol%) Al<sub>2</sub>O<sub>3</sub>–ZrO<sub>2</sub> nanocrystalline powders. The aims of this study was to (i) obtain alumina–zirconia

\* Corresponding author. Tel.: +90 2742652032; fax: +90 2742652066.

E-mail address: [hasangocmez@yahoo.com](mailto:hasangocmez@yahoo.com) (H. Gocmez).

composites powders with soft agglomeration and (ii) examine hardness and toughness of these fabricated composite powders.

## 2. Experimental procedure

For the synthesis of alumina–zirconia with 2 mol% yttria (80/20 vol%) nanocomposite powders, aluminum nitrate (Aldrich 99%), zirconium oxychloride (Fluka 99%) and  $\text{YCl}_3$  (Fluka 99%) were chosen as ceramic precursors. Absolute ethanol (Fluka, analytic reagent) and  $\text{CO}_2$  were used as the solvent and antisolvent, respectively. Precursors were dissolved in ethanol and stirred at room temperature for an hour till a pH value of about 1 was obtained. The supercritical  $\text{CO}_2$  synthesis was conducted by using stainless steel vessel with Teflon liner, equipped with a magnetic stirrer (Model 4575, Parr Instruments, Moline, IL). The reactor system consists of three main parts: high pressure vessel ( $P_{\text{max.}} = 350$  Bar), high pressure  $\text{CO}_2$  pump (Scientific Systems, Model SC-24) for injecting liquid  $\text{CO}_2$  to vessel and controller unit. The prepared solution was placed into Teflon lined 314 stainless steel vessel of 500  $\text{cm}^3$  internal volume and subsequently heated. At the same time, with injection of  $\text{CO}_2$  into vessel by pump, the pressure in vessel was increased to desired value. Supercritical treatments were performed in a temperature range from 100 to 200 °C with the pressure range from 150 to 200 bar for 30 min. The powders named as AZ-1 (150 °C, 15 MPa), AZ-2 (150 °C, 20 MPa) and AZ-3 (200 °C, 20 MPa) were obtained using 30 min at the supercritical condition. The solution in the vessel was mixed by a magnetic stirrer at 100 rpm through experiment. Schematic diagram of the process for supercritical synthesis is showed in Fig. 1.

After synthesis, the dried powders were gently crushed in an agate mortar and repeatedly washed with distilled water, and then suspensions were centrifuged at 9000 rpm for 2 min and dried in an oven at 100 °C. Heat treatment for synthesized powders was carried out to powders at 1000 °C and 1500 °C for 2 h. The powders calcined at 1000 °C for 2 h were compacted into disc (with 13 mm in diameter and 5 mm in height) at a maximum applied pressure of 200 MPa and subsequently sintered at 1600 °C for 5 h in air with a heating and cooling rate of 10 °C/min.

The phase content of the  $\text{Al}_2\text{O}_3$ – $\text{ZrO}_2$  composite powders were identified by X-ray diffractometer (Rigaku, Miniflex) using  $\text{Cu K}\alpha$  radiation over the range of 20–80° at a rate of 2°/min. The crystalline size ( $d_{\text{XRD}}$ ) was calculated from the Scherrer formula [16]. The morphology and microstructure of the sintered discs was studied by polishing the surface with

diamond paste, thermally etching at 1250 °C for 5 h, were gold coated and observed in a field emission scanning electron microscopy (SEM, Zeiss Supra 50 VP). The nanocrystal images of the calcined powders were examined using transmission electron microscopy (TEM, Jeol JEM-2010F) at an acceleration voltage of 200 kV. The specimens were prepared by slow evaporation of a drop of the sample suspension deposited onto a copper grid with carbon film. The surface area of the powders was measured by using BET instrument (Quantachrome Nova 2200 E). Prior to the  $\text{N}_2$  adsorption, the powders were degassed in a vacuum at 200 °C for 2 h. The average particle size (in nanometer) of calcined powders from BET results which is called  $d_{\text{BET}}$  was calculated. The density of the powders was determined using by helium gas pycnometers (Quantachrome Ultrapyc 1200e). The degree of agglomeration was calculated [16]. The relative density of the sintered ceramics was measured using the Archimede's method. Vickers hardness was measured using a static microhardness tester (Future-tech). Before hardness measurements, the samples were mounted with epoxy resin and surface damage was removed mechanically by grinding with 2400 and 4000 grit, and then polishing on 6, 3 and 1  $\mu\text{m}$  diamond lap wheels. Hardness measurement was made at 9.8 N load with a loading time of 15 s. The indentation diagonal lengths were measured Nikon MA 100 inverted metal microscope using Clemex Professional microscopy image analysis software. 50 $\times$  and 20 $\times$  objective lenses were used on the Nikon MA 100 instrument. In view of the scatter of the micro-hardness data, the hardness value was a mean of at least six measurements under the same condition. The hardness values ( $H_V$ ) from the length of the two diagonals of the square-shaped Vickers indents were calculated with the equation:

$$H_V = 1.854 \left( \frac{P}{D} \right)^2$$

where  $P$  is the applied force (in Newton) and  $d$  the diagonal length (in mm) of the indentation.

The value of the hardness at 9.8 N and extended corner cracking was used to calculate the fracture toughness ( $K_{\text{IC}}$ ) with the Evans [17] and Anstis et al. [18] methods. A value of 350 GPa, which is the elastic modulus of ZTA ( $\text{Al}_2\text{O}_3$ –20 vol%  $\text{ZrO}_2$ ), was used in calculation of fracture toughness.

## 3. Results and discussion

Fig. 2(a–c) shows X-ray diffraction traces of as-synthesized and calcined AZ-1 powders. As-synthesized powder consists of

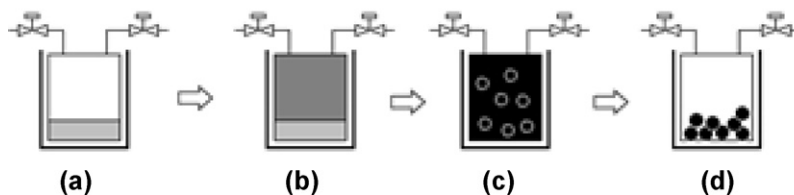


Fig. 1. Schematic diagram of the process for supercritical synthesis. (a) Solution consisting of precursor and solvent (b) injecting  $\text{CO}_2$  into vessel to get desired pressure and heating  $P < P_{\text{critic}} - T < T_{\text{critic}}$  (c) precipitate formation under the supercritic condition  $P > P_{\text{critic}} - T > T_{\text{critic}}$  (d) venting  $P = 1$  atm.

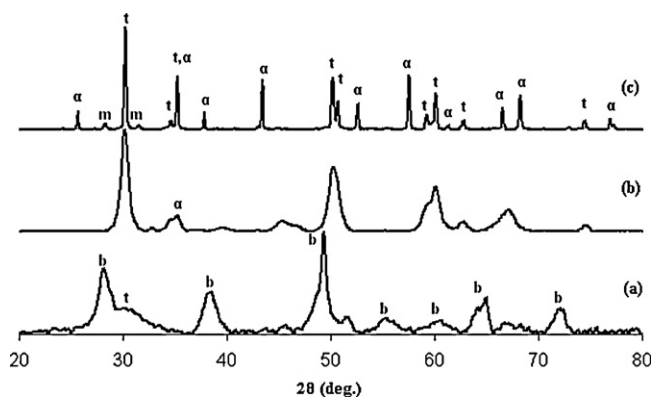


Fig. 2. (a–c) XRD traces showing phase evolution of AZ-1 composite powder calcined at different temperatures (a) RT, (b) 1000 °C, (c) 1500 °C (t and m: tetragonal and monoclinic zirconia respectively, b: boehmite, α: alumina).

boehmite,  $\text{AlO}(\text{OH})$ , with minor tetragonal zirconia (Fig. 2a). After heat treatment at 1000 °C, tetragonal zirconia ( $\text{t-ZrO}_2$ ) as major phase and  $\alpha$ -alumina are formed as major and minor phases, respectively (Fig. 2b). After calcining at 1500 °C the tetragonal zirconia and  $\alpha$ -alumina are the dominant phases with a small amount of monoclinic zirconia. The crystallite size of tetragonal zirconia and  $\alpha$ -alumina increased with temperature from 10 to 49 nm and from 16 to 69 nm at 1000 °C and 1500 °C, respectively.

The pressure and temperature are important parameters effecting the nucleation and growth during the supercritical particle formation period. The crystal size of alumina powders (Table 1) decreased from 16 to 6 nm with increasing temperature and pressure since the increasing of crystallite size for the samples upon rising of temperature triggered phase changes of zirconia (tetragonal to monoclinic), which suppressed growth of alumina at the same volume. In addition, the increase in temperature pressure caused a large supersaturation and decrease in the free energy barrier and thus the nucleation rate was accelerated in which the crystalline size became smaller.

It is well known that the monoclinic phase of zirconia is the stable phase at low temperatures, however, the tetragonal phase is the first formed upon heat treatment. Tetragonal phase formation is frequently attributed to several factors such as chemical effects, structural similarities between the tetragonal phase and the amorphous phase of precursors as well as particle size effects. Furthermore, the presence of lattice strains and defect centers on crystalline structure do not allow the tetragonal to monoclinic transformation in the free powder state to occur below a certain particle size ( $< \sim 30$  nm) [19]. The stability of  $\text{t-ZrO}_2$  can also be achieved by dopants such as  $\text{CaO}$ ,  $\text{MgO}$ ,  $\text{Y}_2\text{O}_3$ ,  $\text{CeO}_2$ , etc. In this study, the 2 mol% yttria

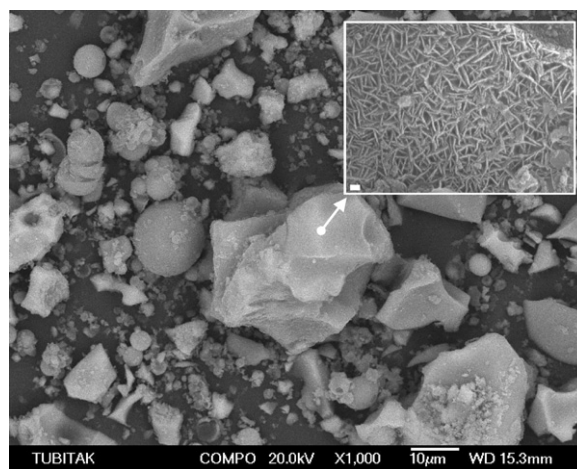


Fig. 3. SEM image of the AZ-3 as-prepared nanocrystalline composite powders (bar: 100 nm).

doped - zirconia particles are dispersed into the alumina matrix, which also hindered the transformation of tetragonal to monoclinic phase [20].

The results of surface area, density, particle size and crystallite size of the  $\text{Al}_2\text{O}_3$ – $\text{ZrO}_2$  powder synthesized from different supercritical conditions are shown in Table 1. All powder was calcined at 1000 °C for 2 h. It is evident that the changes of temperature and pressure during the synthesis have an important effect on the final powder properties. As both of temperature and pressure are increased, the density, surface area and agglomeration degree increase, whereas crystallite size and in case of AZ-3 particle size decreased. When only the pressure is increased from 15 MPa to 20 MPa (AZ-2), the same results as for AZ-3 are obtained except that the degree of agglomeration is less than that of AZ-3. The lower agglomeration leads to powders with less or softer agglomerated clusters. It was observed that the pressure was a more effective parameter than temperature during the supercritical synthesis. The results clearly show that tunable properties of supercritical fluid such as temperature and pressure can be used to produce powders with different characteristics (size, morphology, etc.)

The particles at various morphologies were observed in the SEM micrograph of as-received sample (Fig. 3). At high magnification in the SEM, it can be seen that large powder consists of primary particle having nanosize and plate-like in shape. Crystals with needle shape are seen in TEM images of as prepared AZ-1 (Fig. 4). The agglomeration degrees (N) for powders are changed from 1.2 and 5.4. As the value N becomes smaller or N value is close to unity, agglomerates tend to be approached their primary particle size, which may be defined as

Table 1

The characteristics of calcined at 1000 °C for 2 h  $\text{Al}_2\text{O}_3$ –20 vol%  $\text{ZrO}_2$  powders synthesized under the different supercritical conditions.

Sample	Density ( $\text{g}/\text{cm}^3$ )	Surface area ( $\text{m}^2/\text{g}$ )	Crystallite size of $\text{Al}_2\text{O}_3$ from XRD (nm)	Particle size from BET (nm)	Agglomeration degree, $N (d_{\text{BET}}^3/d_{\text{XRD}}^3)$
AZ-1	3.52	86	15.7	19.8	2.01
AZ-2	4.08	93	14.8	15.8	1.22
AZ-3	4.00	150	5.7	10.00	5.40

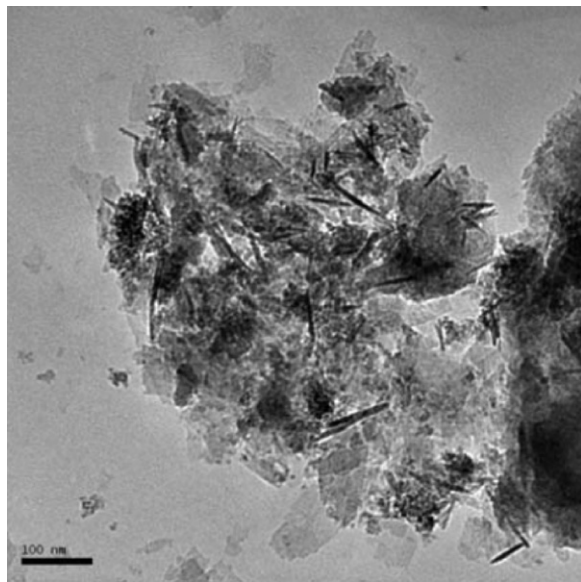


Fig. 4. TEM image of the AZ-1 as-prepared nanocrystalline composite powders.

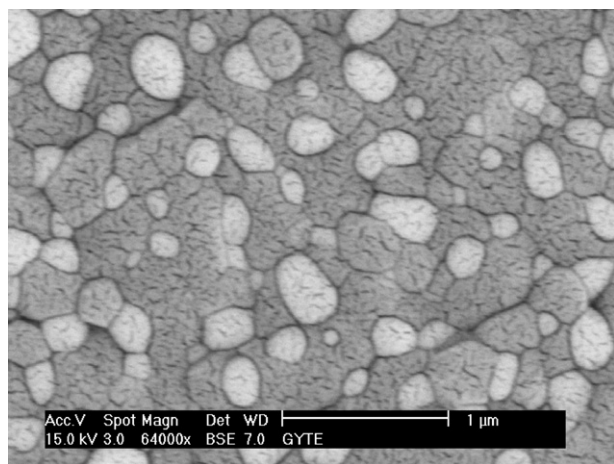


Fig. 5. SEM microstructure of sintered ceramic from AZ-2 powder at 1600 °C for 5 h. The dark and white grains show  $\text{Al}_2\text{O}_3$  and  $\text{ZrO}_2$  particles, correspondingly (addition detail is notification of the thick Au coating).

loose powders or softly agglomerated powders. It is crucial to achieve soft or few agglomerated powders for optimizing powder compaction, sintering characteristics and engineering properties.

SEM micrographs (backscatter image) shown in Fig. 5 present the microstructure of sintered ceramic produced from

AZ-2 powder having the lowest agglomeration degree fired at 1600 °C for 5 h. After sintering, the relative density of specimen was found to be 98.9% of the theoretical. A homogeneous dispersion of zirconia grains (bright phase) in alumina matrix (dark phase) was obtained, which shows homogenous microstructure in nanoscale (the finer crack-like features on SEM micrographs occurred as a result of too thick a gold coating of samples in Fig. 5.). The grain size of zirconia has a wide range (100–500 nm) while that of alumina has larger than zirconia one. It is clear that alumina prevents tetragonal – monoclinic transformation of zirconia on cooling by compressing it at the triple point of alumina. As is known, the tetragonal – monoclinic phase transformation can act as a mechanism which enhances the toughness in mechanical application of the alumina–zirconia composites.

The hardness and fracture toughness of the sintered ceramic produced from AZ-2 powders are given in Table 2. The hardness values for the sintered samples were measured to be 12.5 GPa under the 9.8 N load. The fracture toughness for Anstis and Evans were found to be 3.4 and 3.1  $\text{MPam}^{1/2}$ , respectively. The diverse values of hardness for ZTA materials in literature have been presented. These differences of hardness values are attributed to processing conditions (sintering and forming method), amount of phases, particle size as well as the measurement techniques of hardness. The hardness values such as 12–14 [21,22] or 19 GPa [23,24] were obtained by hot pressing whereas the hardness of ZTA (zirconia toughened alumina) formed using colloidal techniques was reported as 15 GPa.

#### 4. Summary

Nanocrystalline ZTA composite powders containing 20 vol% zirconia were successfully synthesized using the supercritical  $\text{CO}_2$  method. The effect of synthesis temperature and pressure were studied as a function of the powder properties achieved. The study has shown that supercritical conditions such as pressure and temperature influence the morphology and degree of agglomeration in the powders. It can be stated that the synthesized particles consist of mostly primary particles with less agglomeration when compared with powders synthesis by traditional techniques. Hence, the supercritical  $\text{CO}_2$  method can be tailored to successfully control the degree of agglomeration during nanocrystalline powders synthesis of ZTA composite powders. Alumina grains as well as yttria addition hindered tetragonal–monoclinic phase transformation of zirconia by compressing it at the triple point of alumina.

Table 2

The density, vickers hardness and fracture toughness of composite sintered at 1600 °C for 5 h.

Sintering temperature (°C)	Relative density (%)	Hardness [GPa] under the 9.8 N load	Fracture toughness $K_{IC}$ [ $\text{MPam}^{1/2}$ ]	
			Antis	Evans
1600	98.9	12.5	3.4	3.1



## Acknowledgements

The financial supports provided by the Scientific and Technological Research Council of Turkey (TUBITAK, project no: 107M367) are gratefully acknowledged. The authors also would like to thank research foundation of Mustafa Kemal University (grant no: 08 F 0501) for mechanical measurements.

## References

- [1] M. Yoshimura, S. Tag Oha, M. Sandob, K. Niihara, Crystallization, Microstructural characterization of  $\text{ZrO}_2$  (3 mol%  $\text{Y}_2\text{O}_3$ ) nano-sized powders with various  $\text{Al}_2\text{O}_3$  contents, *J. Alloys Compd.* 290 (1999) 284–289.
- [2] M. Weimin, W. Lei, G. Renguo, S. Xudong, L. Xikun, Sintering densification, microstructure and transformation behavior of  $\text{Al}_2\text{O}_3/\text{ZrO}_2$  composites, *Mater. Sci. Eng. A* 477 (2008) 100–106.
- [3] J.F. Bartolomé, A.H. De Aza, A. Martín, J.Y. Pastor, J. Llorca, R. Torrecillas, G. Bruno, Alumina/zirconia micro/nanocomposites: a new material for biomedical applications with superior sliding wear resistance, *J. Am. Ceram. Soc.* 90 (10) (2007) 3177–3184.
- [4] D. Enache, M. Roy-Auberger, K. Esterle, R. Revel, Preparation of  $\text{Al}_2\text{O}_3$ – $\text{ZrO}_2$  mixed supports; their characteristics and hydrothermal stability, *Colloids Surf. A Physicochem. Eng. Asp.* 220 (2003) 223–233.
- [5] I.A. Aksay, F.F. Lange, B.I. Davis, Uniformity of  $\text{Al}_2\text{O}_3$ – $\text{ZrO}_2$  composites by colloidal filtration, *J. Am. Ceram. Soc.* 66 (10) (1983) 190–192.
- [6] J. Chandradass, K.H. Kim, Effect of acidity on the citrate–nitrate combustion synthesis of alumina–zirconia composite powder, *Met. Mater. Int.* 15 (6) (2009) 1039–1043.
- [7] Y. Murase, E. Kato, K. Daimon, Stability of  $\text{ZrO}_2$  phases in ultrafine  $\text{ZrO}_2$ – $\text{Al}_2\text{O}_3$  mixtures, *J. Am. Ceram. Soc.* 69 (2) (1986) 83–87.
- [8] S. Hori, M. Yoshimura, S. Somiya, R. Takahashi,  $\text{Al}_2\text{O}_3$ – $\text{ZrO}_2$  ceramics prepared from CVD powders, in: N. Claussen, M. Ruhle, A.H. Heuer (Eds.), *Advances in Ceramics Science and Technology of Zirconia II*, vol. 12, The American Ceramic Society, Columbus, Ohio, 1984 pp. 794–880.
- [9] A. Saha, D.C. Agrawal, Microstructure development in hybrid sol–gel prepared  $\text{Al}_2\text{O}_3$ – $\text{ZrO}_2$  composites, *J. Mater. Sci. Lett.* 17 (1998) 1333–1336.
- [10] D.W. Watson, R.D. Smith, Supercritical fluid technologies for ceramic-processing application, *J. Am. Ceram. Soc.* 72 (6) (1989) 871–881.
- [11] A. Hertz, S. Sarrade, C. Guizard, A. Julbe, J.-C. Ruiz, B. Fumel, Synthesis, Encapsulation with a polymer of nanophase YSZ particles in supercritical  $\text{CO}_2$ , *Rev. Adv. Mater. Sci.* 10 (2005) 176–180.
- [12] F. Cansell, C. Aymonier, A. Loppinet-Serani, Review on material science and supercritical fluids, *Curr. Opin. Solid State Mater. Sci.* 7 (2003) 331–340.
- [13] A. Hertz, S. Sarrade, C. Guizard, A. Julbe, Synthesis, Encapsulation of yttria stabilized zirconia particles in supercritical carbon dioxide, *J. Eur. Ceram. Soc.* 26 (7) (2006) 5–1203.
- [14] E. Reverchon, R. Adami, Nanomaterials and supercritical fluids, *J. Supercrit. Fluids* 37 (2006) 1–22.
- [15] C. Aymonier, A. Loppinet-Serani, H. Reverón, Y. Garrabos, François Cansell, Review of supercritical fluids in inorganic materials science, *J. Supercrit. Fluids* 38 (2006) 242–251.
- [16] M. Winterer, *Nanocrystalline Ceramics – Synthesis and Structure*. Springer Series in Materials Science, Vol. 53, Springer Verlag, NY, 2002 p. 24.
- [17] A.G. Evans, Fracture toughness: the role of indentation techniques, in: S.W. Freiman (Ed.), *Fracture Mechanics Applied to Brittle Materials* ASTM STP 678, Vol. 11, American Society for Testing and Materials, Blakelysburg, 1979, pp. 2–135.
- [18] G.R. Anstis, P. Chantikul, B.R. Lawn, D.B. Marshall, A critical evaluation of indentation techniques for measuring fracture toughness: i, direct crack measurement, *J. Am. Ceram. Soc.* 64 (9) (1981) 533–538.
- [19] M.W. Pitcher, S.V. Ushakov, A. Navrotsky, Energy crossovers in nanocrystalline zirconia, *J. Am. Ceram. Soc.* 88 (2005) 160–167.
- [20] B.W. Kibble, A.H. Heuer, in: N. Claussen, M. Ruhle, A.H. Heuer (Eds.), *Advances in Ceramics, Science and Technology of Zirconia II*, Vol. 12, The ACerS Inc., Columbus, Ohio, 1984, p. 415.
- [21] J. Hong, L. Gao, S.D.D.L. Torre, H. Miyamoto, K. Miyamoto, Spark plasma sintering and mechanical properties of  $\text{ZrO}_2(\text{Y}_2\text{O}_3)$ – $\text{Al}_2\text{O}_3$  composites, *Mater. Lett.* 43 (2000) 27–31.
- [22] B.T. Lee, K.H. Kim, J.K. Han, Microstructures and material properties of fibrous  $\text{Al}_2\text{O}_3$ –(m- $\text{ZrO}_2$ )/t- $\text{ZrO}_2$  composites fabricated by a fibrous monolithic process, *J. Mater. Res.* 19 (2004) 3234–3241.
- [23] N.L. Hecht, S.M. Goodrich, D.E. McCullum, P.P. Yaney, S.D. Jang, V.J. Tennery, Studies of transformation-toughened ceramics, *Am. Ceram. Soc. Bull.* 71 (6) (1992) 955–959.
- [24] NIST the Webbook for Structural Ceramic, <http://www.ceramics.nist.gov>.